Proceedings of the 3rd International Conference on
Fracture Fatigue and Wear, pp. 57-62, 2014

ANALYSIS OF INTENSITY OF SINGULAR STRESS FIELD FOR SINGLE LAP JOINT UNDER TENSILE SHEAR LOAD BASED ON CRACK TIP STRESS METHOD

Tatsujiro Miyazaki[1], Nao-Aki Noda[2], Rong Li[3], Takumi Uchikoba[3] and Yoshikazu Sano[2]

[1] University of the Ryukyus, Okinawa, Japan
[2] Kyushu Institute of Technology, Fukuoka, Japan
[3]Graduate School of Engineering, Kyushu Institute of Technology, Fukuoka, Japan

Abstract: In this paper, the crack tip stress method (CTSM) is extended so that the intensity of the singular stress field of the single lap joint (SLJ) with two real stress singularity orders can be analyzed. Two types of the reference models are proposed; one is the tensile force model; the other one is the shear force model. The intensities of the singular stress field of the SLJ are calculated by superposing those of the reference models. The intensities of the singular stress fields of the reference models are calculated by the reciprocal work contour integral method (RWCIM). Then the validity of the reference models and the accuracy of the present method are discussed by comparing the present results with the solutions which are calculated by the RWCIM.

Keywords: intensity of singular stress field; FEM; single lap joint; crack tip stress method

1 INTRODUCTION

In recently years, single lap joints (SLJs) have been widely used to bond dissimilar material members particularly in aircraft and automobile structures. The authors reported that debonding fracture criterion of the SLJs can be expressed with the critical intensity of the singular stress field. However, it is not easy to calculate the intensity of the singular stress field of the SLJ.

Nisitani et al. developed the crack tip stress method (CTSM) [1,2] in order to solve the elastic problems with the notch and crack. Then, the CTSM was extended so that the interface crack and interface corner edge can be analyzed. The authors applied the CTSM to the SLJ and analysed the singular stress field at the interface corner edge of the SLJ under the tensile shear load [3, 4]. In the earlier study, the SLJ is used as the reference model. However, when the various SLJs are analyzed, the simple reference model is desired.

In this study, the reference model suitable for the analysis of the SLJ is examined. Then, the intensities of the singular stress field are solved by the CTSM and the reciprocal work contour integral method (RWCIM) [5]. The intensities of the singular stress field are compared, and the validity of the present reference model and the accuracy of the CTSM are examined.

2 CRACK TIP STRESS METHOD

Figure 1 shows the schematic illustration of the SLJ model and boundary condition. l_1 and t_1 are adherend length and adherend thickness, respectively; l_2 and t_2 are overlap length and adhesive thickness, respectively; E is Young's modulus, ν is Poisson's ratio, and subscripts 1 and 2 refer to the adherend and the adhesive, respectively.

The singular stress field is formed at the corner edge of the interface between the adherend and the adhesive. The singular stress field is governed by the order of stress singularity, $\lambda-1$. The eigenvalue λ can be obtained by solving the eigenvalue equation, which was derived by Bogy. In the case of the corner edge as shown in Fig. 1, the eigenequation is given by the following equation [6,7].

$$4\sin^2(\pi\lambda)\left\{\sin^2\left(\frac{\pi\lambda}{2}\right)-\lambda^2\right\}\beta^2+4\lambda^2\sin^2(\pi\lambda)\alpha\beta+\left\{\sin^2\left(\frac{\pi\lambda}{2}\right)-\lambda^2\right\}\alpha^2$$
$$-4\lambda^2\sin^2(\pi\lambda)\beta-2\left\{\lambda^2\cos(2\pi\lambda)+\sin^2\left(\frac{\pi\lambda}{2}\right)\cos(\pi\lambda)+\frac{1}{2}\sin^2(\pi\lambda)\right\}\alpha+\sin^2\left(\frac{3\pi}{2}\lambda\right)-\lambda^2=0 \quad (1)$$

Here, α and β are Dundurs' parameters [8] and defined as follows

$$\alpha=\frac{G_2(\kappa_1+1)-G_1(\kappa_2+1)}{G_2(\kappa_1+1)+G_1(\kappa_2+1)},\ \beta=\frac{G_2(\kappa_1-1)-G_1(\kappa_2-1)}{G_2(\kappa_1+1)+G_1(\kappa_2+1)},\ \kappa_m=\frac{3-\nu_m}{1+\nu_m}(\text{plain stress}),\ 3-4\nu_m(\text{plain strain}) \quad (2)$$

Here, G_m ($m=1,2$) is the shear modulus of elasticity.

The stresses at a radial distance r from the point O on the interface, σ_θ and $\tau_{r\theta}$, are expressed as follows.

$$\sigma_\theta=\frac{K_1}{r^{1-\lambda_1}}f_{\theta\theta}(0,\lambda_1)+\frac{K_2}{r^{1-\lambda_2}}f_{\theta\theta}(0,\lambda_2)=\frac{K_{\sigma,\lambda_1}}{r^{1-\lambda_1}}+\frac{K_{\sigma,\lambda_2}}{r^{1-\lambda_2}},\ \tau_{r\theta}=\frac{K_1}{r^{1-\lambda_1}}f_{r\theta}(0,\lambda_1)+\frac{K_2}{r^{1-\lambda_2}}f_{r\theta}(0,\lambda_2)=\frac{K_{\tau,\lambda_1}}{r^{1-\lambda_1}}+\frac{K_{\tau,\lambda_2}}{r^{1-\lambda_2}} \quad (3)$$

Here, K_1 and K_2 are real numbers, $f_{\theta\theta}(\theta,\lambda_k)$ and $f_{r\theta}(\theta,\lambda_k)$ are non-dimensional functions of the angle θ, λ_k, Dundurs' parameters (α,β). Because four intensities of the singular stress field, K_{σ,λ_1}, K_{σ,λ_2}, K_{τ,λ_1} and K_{τ,λ_2} are determined by two real numbers K_1 and K_2, the singular stress field in the vicinity of the corner edge is also determined by them. In this paper, four intensities of the singular stress field are analyzed by the CTSM.

In this paper, two reference models as shown in Fig. 2 are introduced in consideration of the mechanical condition at the interface corner O in Fig.1. (a) is the tensile force model; (b) is the shear force model. When $T=T_0$ and $S=S_0$,the singular stress field near the interface corner edge of the SLJ is reproduced. In the CTSM, when the reference models and unknown model are analyzed by FEM, the same mesh pattern and the same materials are used as shown in Figs 2 and 3. The stresses at the interface corner edge, $\sigma_{y0,FEM}^{SLJ}$ and $\tau_{xy0,FEM}^{SLJ}$, are expressed as follows.

$$\sigma_{y0,FEM}^{SLJ}=T_0\,\sigma_{y0,FEM}^{T}\big|_{T=1}+S_0\,\sigma_{y0,FEM}^{S}\big|_{S=1}$$
$$\tau_{xy0,FEM}^{SLJ}=T_0\,\tau_{xy0,FEM}^{T}\big|_{T=1}+S_0\,\tau_{xy0,FEM}^{S}\big|_{S=1} \quad (4)$$

Here, $\sigma_{y0,FEM}^{T}|_{T=1}$ and $\tau_{xy0,FEM}^{T}|_{T=1}$ are stresses at the interface corner edge of the tensile force model under $T=1$ by FEM, $\sigma_{y0,FEM}^{S}|_{S=1}$ and $\tau_{xy0,FEM}^{S}|_{S=1}$ are stresses at the interface corner edge of the shear force model under $S=1$ by FEM. The loads T_0 and S_0 can be obtained by solving the simultaneous equation (4). Then, the intensities of the singular stress field of the SLJ can be obtained by superposing the intensities of the singular stress fields of the two reference models as follows.

$$K_{\sigma,\lambda_k}^{SLJ}=T_0\,K_{\sigma,\lambda_k}^{T}\big|_{T=1}+S_0\,K_{\sigma,\lambda_k}^{S}\big|_{S=1}$$
$$K_{\tau,\lambda_k}^{SLJ}=T_0\,K_{\tau,\lambda_k}^{T}\big|_{T=1}+S_0\,K_{\tau,\lambda_k}^{S}\big|_{S=1} \quad (5)$$

Here, $k=1,2$, $K_{\sigma,\lambda_k}^{T}|_{T=1}$ and $K_{\tau,\lambda_k}^{T}|_{T=1}$ are the intensities of the singular stress field of the tensile force model under $T=1$, $K_{\sigma,\lambda_k}^{S}|_{S=1}$ and $K_{\tau,\lambda_k}^{S}|_{S=1}$ are the intensities of the singular stress field of the shear force model under $S=1$.

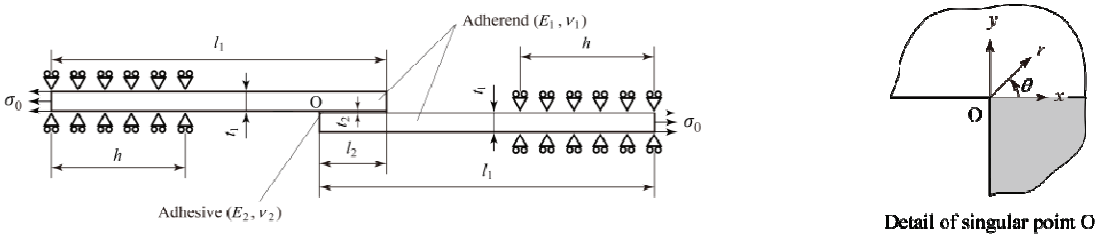

Fig. 1 Schematic illustration of the SLJ

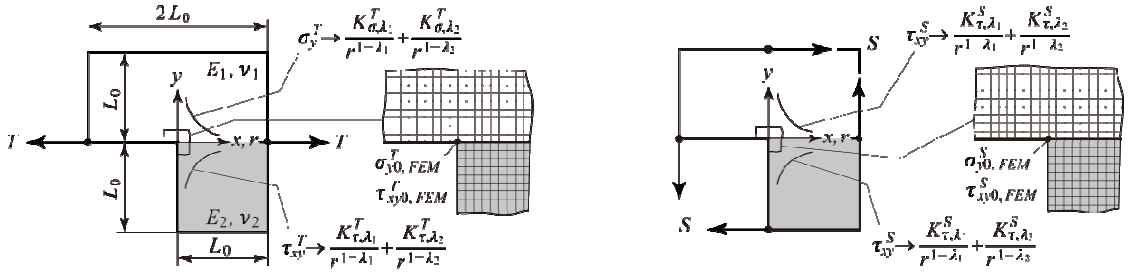

(a) Tensile force model (b) Shear force model

Fig. 2 Reference models used for analysis of SLJ

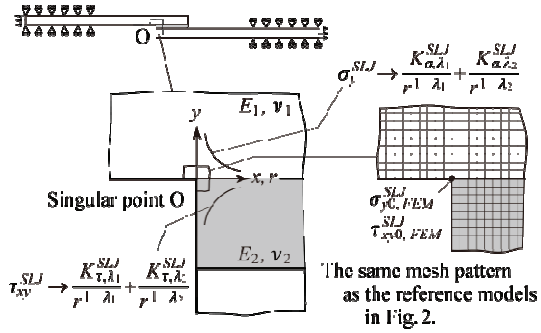

Fig. 3 SLJ model used for analysis

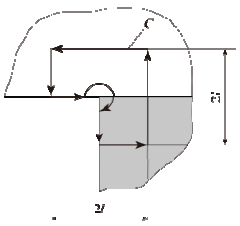

Fig. 4 Contour integral path

3 COMPARISON CTSM WITH RWCIM

In this section, the numerical simulations are performed for four kinds of material combinations: $(\alpha, \beta) = (-0.3, 0.0), (0.3, 0.0), (0.6, 0.0)$ and $(0.8, 0.3)$. In these material combinations, the eigenequation (1) has two different real roots. Then, the validity of the reference models and the accuracy of the CTSM are examined through the simulation results.

The intensities of the singular stress fields of the tensile force model and the shear force model under $L_0 = 1$ mm and $T = S = 1$ N were determined by the RWCIM. The plane strain condition was assumed in the FEM analyses. The commercial FEM code MSC Marc 2008 R1 was used. Figure 4 shows the contour integral path C. Eight node iso-parametric quadrilateral element was used. Table 1 shows the eigenvalues λ_1 and λ_2. Table 2 shows the intensities of the singular stress fields of the reference models.

Table 1 eigenvalues λ_1 and λ_2

Mat. comb.	α	β	λ_1	λ_2
1	-0.3	0.0	0.558760	0.962655
2	0.3	0.0	0.530697	0.821357
3	0.6	0.0	0.517317	0.703330
4	0.8	0.3	0.544319	0.588069

Table 2 Intensities of singular stress field of the reference models

Mat. comb.	Tensile force model				Shear force model			
	K^T_{σ,λ_1}	K^T_{τ,λ_1}	K^T_{σ,λ_2}	K^T_{τ,λ_2}	K^S_{σ,λ_1}	K^S_{τ,λ_1}	K^S_{σ,λ_2}	K^S_{τ,λ_2}
1	0.02303	-0.01225	-0.8423	-0.1162	-0.06735	0.03583	0.04017	0.005542
2	0.02593	-0.01436	-0.3538	-0.1108	-0.05370	0.02973	-0.005941	-0.001860
3	0.02542	-0.01434	-0.1261	-0.05264	-0.04789	0.02701	0.002428	0.001013
4	0.005374	-0.03806	0.001316	0.005596	-0.02639	0.1869	-0.05136	-0.2184

K^T_{σ,λ_k} , K^T_{τ,λ_k} , K^S_{σ,λ_k} , K^S_{τ,λ_k} : MPa $\cdot$ m $^{1-\lambda_k}$

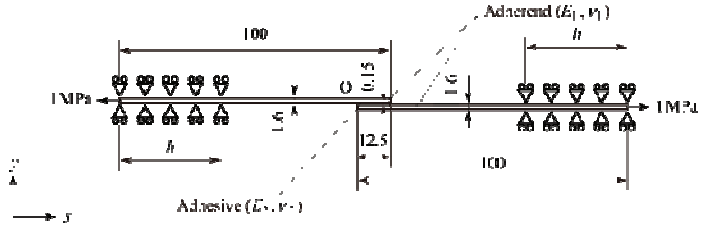

Fig. 5 Analysis model of SLJ (JIS K6850)

Table 3 FEM analysis results of $(\alpha,\beta)=(0.8,0.3)$ when $e_{\min}=3^{-6}$, 3^{-12} and $h=0$

$e_{\min}$	$\sigma^T_{y0,FEM}\big\vert_{T=1}$ $\tau^T_{xy0,FEM}\big\vert_{T=1}$	$\sigma^S_{y0,FEM}\big\vert_{S=1}$ $\tau^S_{xy0,FEM}\big\vert_{S=1}$	$\sigma^{SLJ}_{y0,FEM}$ $\tau^{SLJ}_{xy0,FEM}$	T_0 S_0
3^{-6}	7.217509 -19.25787	-53.96143 46.90953	19.88394 -28.67493	0.8772241 -0.2511529
3^{-12}	143.1043 -396.0553	-982.6654 1223.759	372.3804 -654.7021	0.8766007 -0.2512911

Figure 5 shows the schematic illustration of the SLJ and the boundary conditions. This model is based on JIS K6850. The adhesive thickness $t_2=0.15$ mm, the tensile stress $\sigma_0=1$ MPa, the grip length $h=37.5$ mm were set. In the FEM analyses for RWCIM, eight node iso-parametric quadrilateral element was used near the interface corner edge; four node iso-parametric quadrilateral element was used in the other area. On the other hand, four node iso-parametric quadrilateral element was used in the FEM analyses for CTSM. Table 3 shows the FEM analysis results, T_0 and S_0 . The intensities of the singular stress field of the SLJ are obtained from the T_0 and the S_0 . Figure 6 shows the relative difference between the results of the CTSM and the RWCIM. The relative differences of the $K^{SLJ}_{\sigma,\lambda_1}$ values and the $K^{SLJ}_{\sigma,\lambda_2}$ values are almost constant independent of the element size. Then, there is little difference between the analysis results of the CTMS and the RWCIM

Table 4 shows four intensities of the singular stress field of the SLJ, $K^{SLJ}_{\sigma,\lambda_1}$, $K^{SLJ}_{\sigma,\lambda_2}$, K^{SLJ}_{τ,λ_1} and K^{SLJ}_{τ,λ_2} which were determined by the CTSM and the RWCIM. There is little difference between the analysis results of the CTMS and the RWCIM. Therefore, the accuracy of the CTSM can be confirmed.

As mentioned above, in the CTSM the intensity of the singular stress field of the SLJ can be obtained from the stress values at the interface corner edge of the reference models and the SLJ model which are calculated by FEM under the same material constants and the same mesh pattern. Therefore, when the intensities of the singular stress field of the reference models are solved on the various material

combinations which are presented with Dundurs' parameter (α, β) in advance, the intensity of the singular stress field of arbitrary SLJ can be obtained easily and promptly.

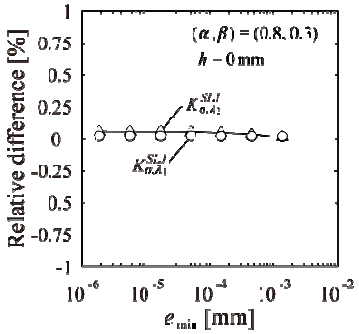

Fig. 6 Relative difference between $K^{SLJ}_{\sigma,\lambda_k}$ values by the present method and RWCIM

Table 4 Intensities of singular stress field when $e_{\min} = 3^{-12}$

(a) $h = 0$ mm

Mat. comb. (α, β)	CTSM		RWCIM	
	$K^{SLJ}_{\sigma,\lambda_1}$	K^{SLJ}_{τ,λ_1}	$K^{SLJ}_{\sigma,\lambda_1}$	K^{SLJ}_{τ,λ_1}
	$K^{SLJ}_{\sigma,\lambda_2}$	K^{SLJ}_{τ,λ_2}	$K^{SLJ}_{\sigma,\lambda_2}$	K^{SLJ}_{τ,λ_2}
1	0.03561	-0.01895	0.03566	-0.01897
(-0.3, 0.0)	-0.7622	-0.1051	-0.7608	-0.1050
2	0.03529	-0.01954	0.03531	-0.01955
(0.3, 0.0)	-0.3012	-0.09434	-0.3009	-0.09423
3	0.03399	-0.01917	0.03400	-0.01918
(0.6, 0.0)	-0.1078	-0.04500	-0.1078	-0.04497
4	0.01134	-0.08034	0.01134	-0.08032
(0.8, 0.3)	0.01406	0.05979	0.01405	0.05975

$K^{SLJ}_{\sigma,\lambda_k}$, K^{SLJ}_{τ,λ_k}, $K^{SLJ}_{\sigma,\lambda_k}$, K^{SLJ}_{τ,λ_k} : MPa · m$^{1-\lambda_k}$

(b) $h = 37.5$ mm

Mat. comb. (α, β)	CTSM		RWCIM	
	$K^{SLJ}_{\sigma,\lambda_1}$	K^{SLJ}_{τ,λ_1}	$K^{SLJ}_{\sigma,\lambda_1}$	K^{SLJ}_{τ,λ_1}
	$K^{SLJ}_{\sigma,\lambda_2}$	K^{SLJ}_{τ,λ_2}	$K^{SLJ}_{\sigma,\lambda_2}$	K^{SLJ}_{τ,λ_2}
1	0.03289	-0.01750	0.03290	-0.01750
(-0.3, 0.0)	-0.7052	-0.09728	-0.7036	-0.09705
2	0.03256	-0.01803	0.03255	-0.01802
(0.3, 0.0)	-0.2801	-0.08772	-0.2797	-0.08758
3	0.03134	-0.01768	0.03133	-0.01767
(0.6, 0.0)	-0.1005	-0.04196	-0.1004	-0.04192
4	0.01034	-0.07326	0.01033	-0.07316
(0.8, 0.3)	0.01261	0.05363	0.01258	0.05352

$K^{SLJ}_{\sigma,\lambda_k}$, K^{SLJ}_{τ,λ_k}, $K^{SLJ}_{\sigma,\lambda_k}$, K^{SLJ}_{τ,λ_k} : MPa · m$^{1-\lambda_k}$

4 CONCLUSIONS

In order to apply the CTSM to the SLJ, the tensile force model and the shear force model were introduced. Then, the validity of two reference models and the accuracy of the CTSM were examined by performing the numerical simulations on JIS type SLJ for $(\alpha, \beta) = (-0.3, 0.0), (0.3, 0.0), (0.6, 0.0)$ and $(0.8, 0.3)$. It was confirmed that four intensities of the singular stress field of the SLJ, $K^{SLJ}_{\sigma,\lambda_1}$, $K^{SLJ}_{\sigma,\lambda_2}$, K^{SLJ}_{τ,λ_1} and K^{SLJ}_{τ,λ_2}, can be obtained by superposing the intensities of the singular stress fields of two reference models. Then, when the results by the CTSM were compared with those by the RWCIM, there is little difference between them.

5 REFERENCES

[1] Nisitani, H., et. al., Determination of Highly Accurate Values of Stress Intensity Factor or Stress Concentration Factor of Plate Specimen by FEM, Trans. Jpn. Soc. Mech. Eng., Ser. A, 65-629 (1999), 26-31.

[2] Zhang, Y., et. al., Effect of Adhesive Thickness on the Interface of Singular Stress at the Adhesive Dissimilar Joint, Trans. Jpn. Soc. Mech. Eng., Ser. A, 77-774 (2011), 360-372.

[3] Noda, N. –A., et. al., Intensity of Singular Stress for Single Lap Joint, Trans. Jpn. Soc. Mech. Eng., Ser. A, 78-789 (2011), 651-655.

[4] Miyazaki, T., et. al., Debonding Criterion for Single Lap Joints from the Intensity of Singular Stress Field, Journal of Japan Institute of Electronics Packaging, 16-2 (2013), 143-151

[5] W. C. Carpenter and C. Byers, A Path Independent Integral for Computing Stress Intensities for V-notched Cracks in a Bimaterial, Int. J. Fract., 35, (1987), 245 - 268.

[6] Bogy, D. B., Edge-bonded dissimilar orthogonal elastic wedges under normal and shear loading, Transaction of the ASME, Journal of Applied Mechanics, Vol. 35, (1968), pp. 460-466.

[7] Bogy, D. B., Two edge-bonded elastic wedges of different and wedge angles under surface tractions, Transaction of the ASME, Journal of Applied Mechanics, Vol. 38, (1971), pp. 377-386.

[8] Dundurs, J., Discussion of edge-bonded dissimilar orthotropic elastic wedges under normal and shear loading, Journal of Applied Mechanics, Vol. 36, (1969), pp. 650-652.